Single Particle Tunneling

If the barrier is sufficiently thin (less than 10 or 20 Å) there is a significant probability that an electron which impinges on the barrier will pass from one metal to the other: this is called **tunneling**.

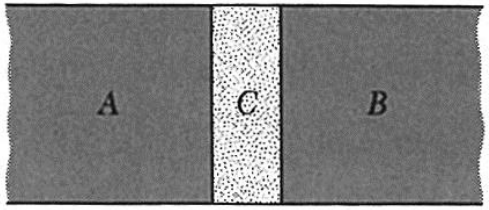

Figure 20 Two metals, *A* and *B*, separated by a thin layer of an insulator *C*.

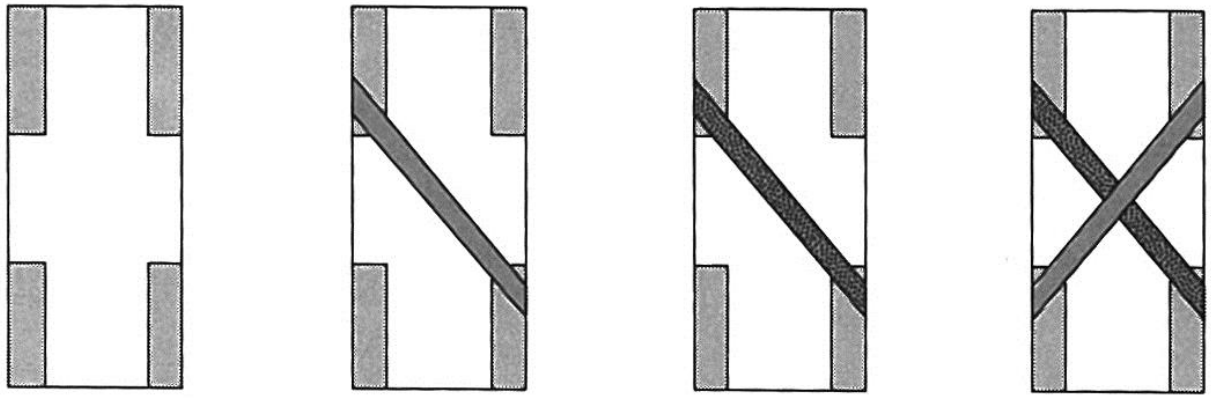

Figure 21 Preparation of an $Al/Al_2O_3/Sn$ sandwich. (a) Glass slide with indium contacts. (b) An aluminum strip 1 mm wide and 1000 to 3000 Å thick has been deposited across the contacts. (c) The aluminum strip has been oxidized to form an Al_2O_3 layer 10 to 20 Å in thickness. (d) A tin film has been deposited across the aluminum film, forming an $Al/Al_2O_3/Sn$ sandwich. The external leads are connected to the indium contacts; two contacts are used for the current measurement and two for the voltage measurement. (After Giaever and Megerle.)

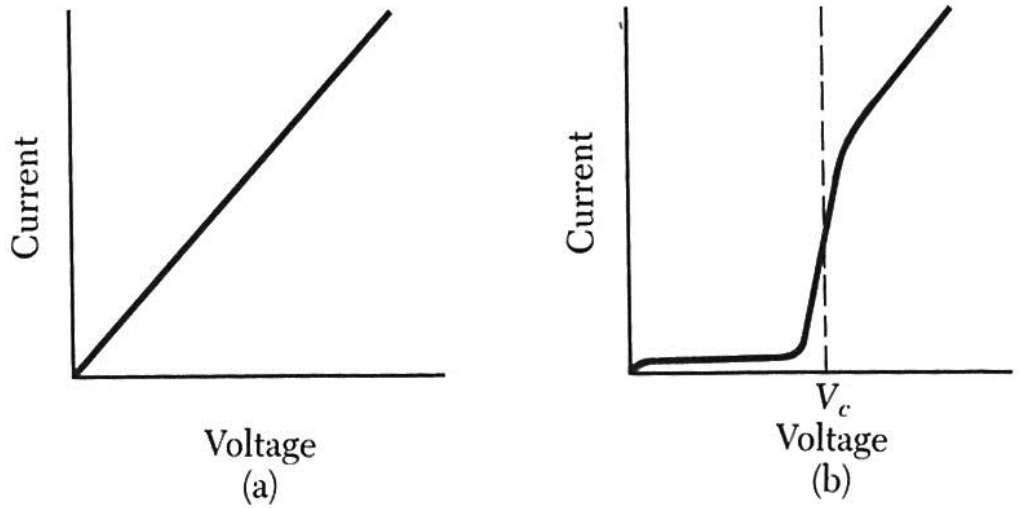

N-N tunneling **S-N tunneling**

Figure 22 (a) Linear current-voltage relation for junction of normal metals separated by oxide layer; (b) current-voltage relation with one metal normal and the other metal superconducting.

1. When both metals are normal conductors, the current-voltage relation of is ohmic at low voltages,

2. Giaever (1960) discovered that if one of the metals becomes superconducting the current-voltage characteristic changes from the straight line of Fig. 22a to the curve shown in Fig. 22b.

Giaever Tunneling

In the superconductor there is an energy gap centered at the Fermi level. At absolute zero no current can flow until the applied voltage is

$$V = E_g/2e = \Delta/e.$$

N (E) = E/ $(E^2-\Delta^2)^{1/2}$

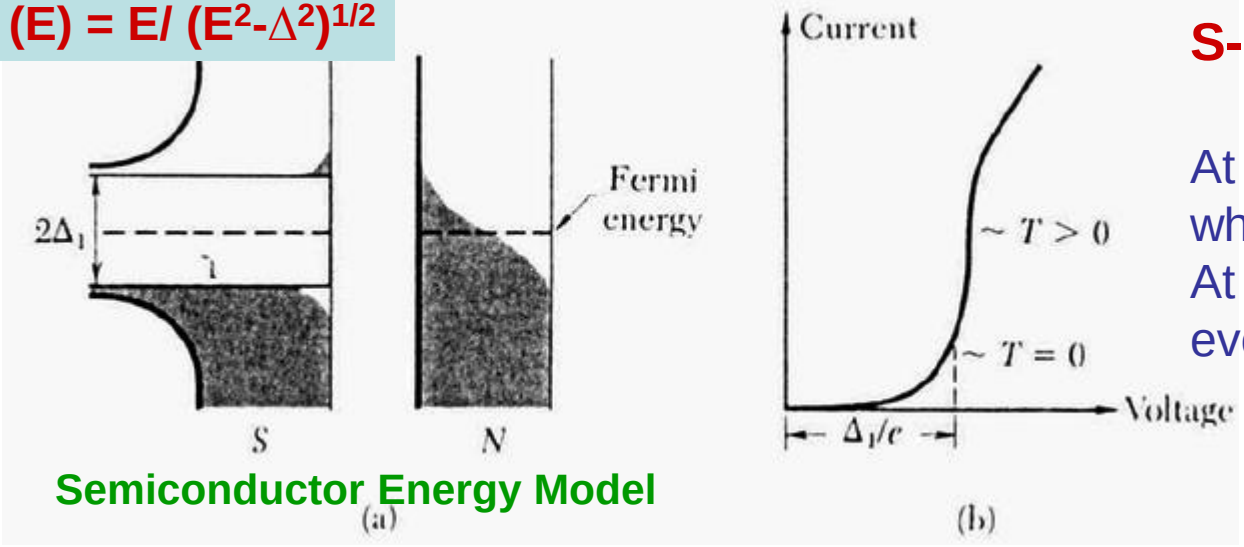

Semiconductor Energy Model

S-N tunneling

At T = 0, **I** is finite when E > Δ,
At T > 0, **I** is > 0 even for E < Δ

Figure 23 The density of orbitals and the current-voltage characteristic for a tunneling junction. In (a) the energy is plotted on the vertical scale and the density of orbitals on the horizontal scale. One metal is in the normal state and one in the superconducting state. (b) I versus V; the dashes indicate the expected break at $T = 0$. (After Giaever and Megerle.)

The current starts when $eV = \Delta$. At finite temperatures because of electrons in the superconductor that are thermally excited across the energy gap.

Josephson Superconductor Tunneling

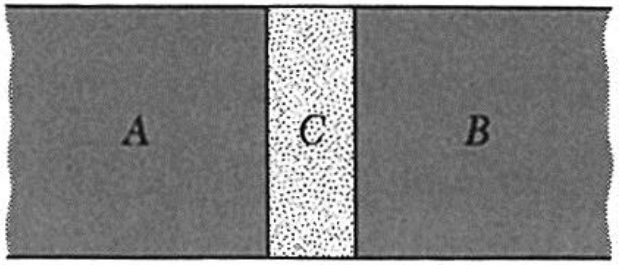

S-I-S
S-N-S

Such a junction is called a weak link.

1. **Dc Josephson effect.** A dc current flows across the junction in the absence of any electric or magnetic field.

2. **Ac Josephson effect.** A dc voltage applied across the junction causes rf current oscillations across the junction.
an rf voltage applied with the dc voltage can then cause a dc current across the junction.

3. **Macroscopic long-range quantum interference.** A dc magnetic field applied through a superconducting circuit containing two junctions causes the maximum supercurrent to show interference effects as a function of magnetic field intensity. SQUID

Dc Josephson Effect. Our discussion of Josephson junction phenomena follows the discussion of flux quantization, let both superconductors be identical.

$$i\hbar \frac{\partial \psi_1}{\partial t} = \hbar T \psi_2 \ ; \qquad i\hbar \frac{\partial \psi_2}{\partial t} = \hbar T \psi_1 \ . \tag{38}$$

Here $\hbar T$ represents the effect of the electron-pair coupling or transfer interaction across the insulator; T has the dimensions of a rate or frequency. It is a measure of the leakage of ψ_1 into the region 2, and of ψ_2 into the region 1.

Let $\psi_1 = n_1^{1/2} e^{i\theta_1}$ and $\psi_2 = n_2^{1/2} e^{i\theta_2}$. Then

$$\frac{\partial \psi_1}{\partial t} = \tfrac{1}{2} n_1^{-1/2} e^{i\theta_1} \frac{\partial n_1}{\partial t} + i\psi_1 \frac{\partial \theta_1}{\partial t} = -iT\psi_2 \ ; \tag{39}$$

$$\frac{\partial \psi_2}{\partial t} = \tfrac{1}{2} n_2^{-1/2} e^{i\theta_2} \frac{\partial n_2}{\partial t} + i\psi_2 \frac{\partial \theta_2}{\partial t} = -iT\psi_1 \ . \tag{40}$$

We multiply (39) by $n_1^{1/2} e^{-i\theta_1}$ to obtain, with $\delta \equiv \theta_2 - \theta_1$,

$$\frac{1}{2} \frac{\partial n_1}{\partial t} + i n_1 \frac{\partial \theta_1}{\partial t} = -iT(n_1 n_2)^{1/2} e^{i\delta} \ . \tag{41}$$

We multiply (40) by $n_2^{1/2} e^{-i\theta_2}$ to obtain

$$\frac{1}{2} \frac{\partial n_2}{\partial t} + i n_2 \frac{\partial \theta_2}{\partial t} = -iT(n_1 n_2)^{1/2} e^{-i\delta} \ . \tag{42}$$

Now equate the real and imaginary parts of (41) and similarly of (42):

For the real part

$$\frac{\partial n_1}{\partial t} = 2T(n_1 n_2)^{1/2} \sin \delta \; ; \qquad \frac{\partial n_2}{\partial t} = -2T(n_1 n_2)^{1/2} \sin \delta \; ; \tag{43}$$

For the imaginary part

$$\frac{\partial \theta_1}{\partial t} = -T\left(\frac{n_2}{n_1}\right)^{1/2} \cos \delta \; ; \qquad \frac{\partial \theta_2}{\partial t} = -T\left(\frac{n_1}{n_2}\right)^{1/2} \cos \delta \; . \tag{44}$$

If $n_1 \cong n_2$ as for identical superconductors 1 and 2, we have from (44) that

$$\frac{\partial \theta_1}{\partial t} = \frac{\partial \theta_2}{\partial t} \; ; \qquad \boxed{\frac{\partial}{\partial t}(\theta_2 - \theta_1) = 0 \; .} \tag{45}$$

The Phase difference is time Independent !

$$\frac{\partial n_2}{\partial t} = -\frac{\partial n_1}{\partial t} \; . \tag{46}$$

the current J of superconductor pairs across the junction depends on the phase difference δ as

$$\boxed{J = J_0 \sin \delta = J_0 \sin (\theta_2 - \theta_1) \; .} \tag{47}$$

J ∝ dN/dt

where J_0 is proportional to the transfer interaction T. The current J_0 is the maximum zero-voltage current that can be passed by the junction. With no applied voltage a dc current will flow across the junction (Fig. 24), with a value between J_0 and $-J_0$ according to the value of the phase difference $\theta_2 - \theta_1$. This is the **dc Josephson effect**.

Josephson Current

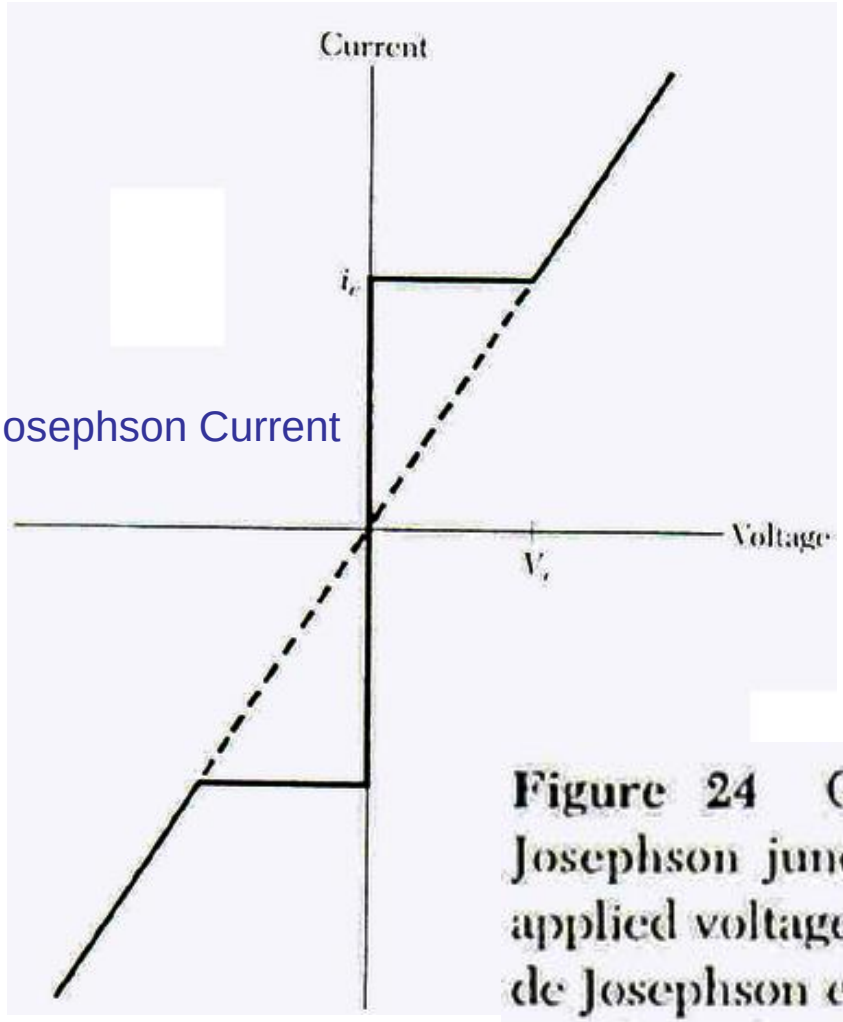

Figure 24 Current-voltage characteristic of a Josephson junction. Dc currents flow under zero applied voltage up to a critical current i_c: this is the dc Josephson effect. At voltages above V_c the junction has a finite resistance, but the current has an oscillatory component of frequency $\omega = 2eV/\hbar$: this is the ac Josephson effect.

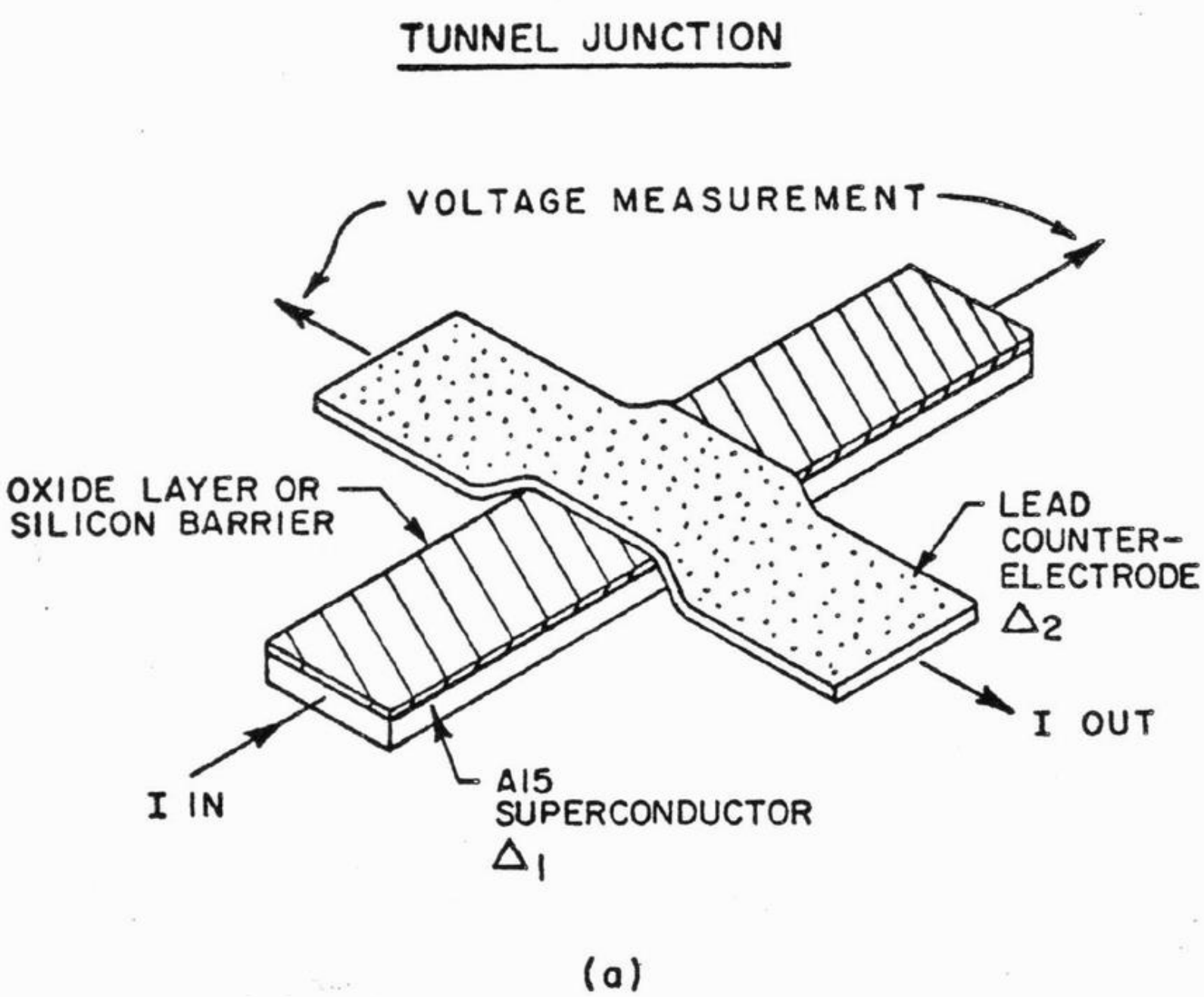

FIG. 1.1--(a) The geometry of our oxide layer tunnel junctions.

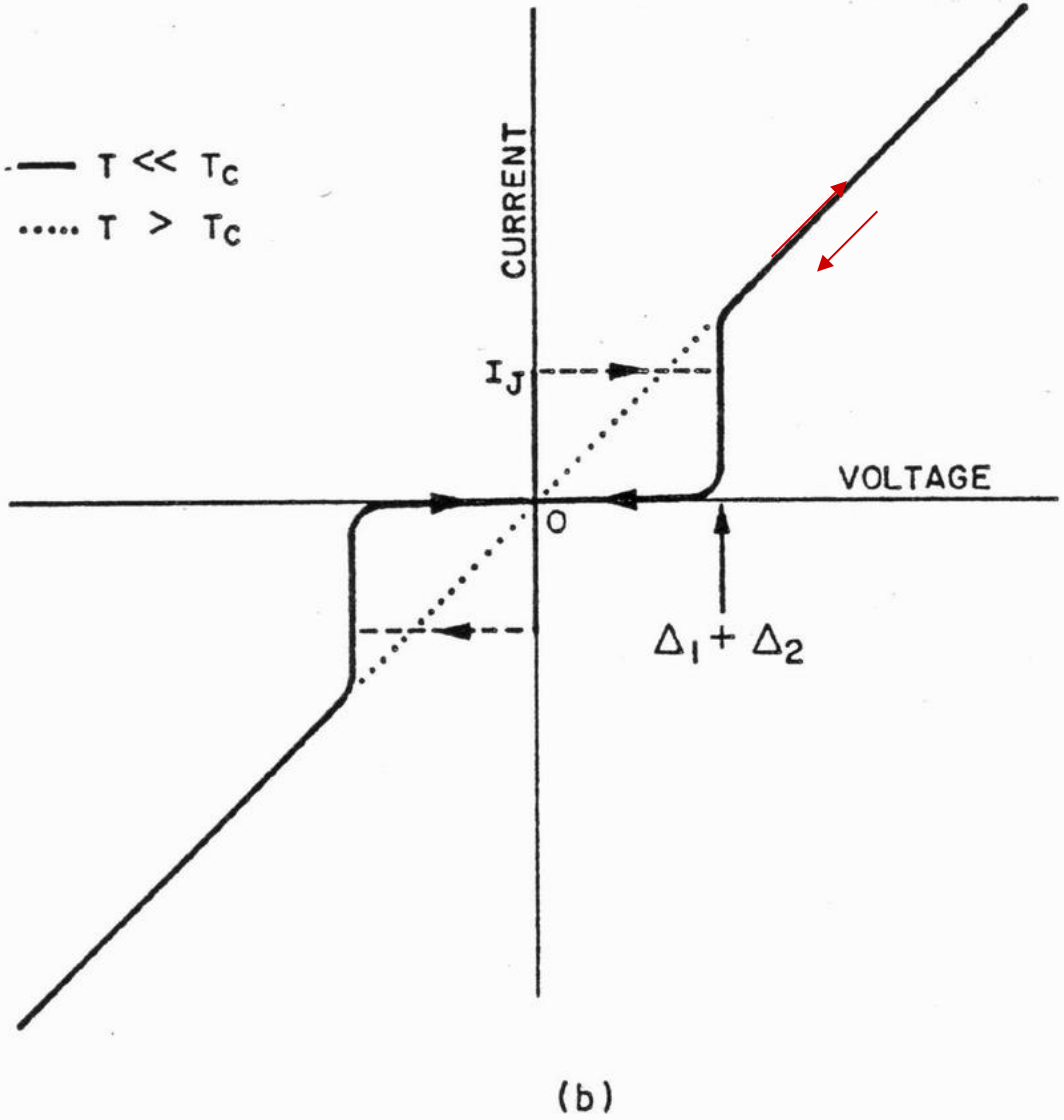

(b)

(b) An idealized current-voltage characteristic showing quasiparticle (Giaever) and pair (Josephson) tunneling through the barrier.

Ac Josephson Effect.

Under a dc voltage V

We can say that a pair on one side is at potential energy $-eV$ and a pair on the other side is at eV.

$$i\hbar\,\partial\psi_1/\partial t = \hbar T\psi_2 - eV\psi_1; \qquad i\hbar\,\partial\psi_2/\partial t = \hbar T\psi_1 + eV\psi_2 \ . \tag{48}$$

Follow Eq. 41

$$\frac{1}{2}\frac{\partial n_1}{\partial t} + in_1\frac{\partial\theta_1}{\partial t} = ieVn_1\hbar^{-1} - iT(n_1n_2)^{1/2}\,e^{i\delta} \ . \tag{49}$$

This equation breaks up into the real part

$$\partial n_1/\partial t = 2T(n_1n_2)^{1/2}\sin\delta \ , \tag{50}$$

exactly as without the voltage V, and the imaginary part

$$\partial\theta_1/\partial t = (eV/\hbar) - T(n_2/n_1)^{1/2}\cos\delta \ , \tag{51}$$

which differs from (44) by the term $eV/\hbar$.

$$\frac{1}{2}\frac{\partial n_2}{\partial t} + in_2\frac{\partial\theta_2}{\partial t} = -i\,eVn_2\hbar^{-1} - iT(n_1n_2)^{1/2}\,e^{-i\delta} \ , \tag{52}$$

$$\partial n_2/\partial t = -2T(n_1 n_2)^{1/2} \sin \delta \ ; \tag{53}$$

$$\partial \theta_2/\partial t = -(eV/\hbar) - T(n_1/n_2)^{1/2} \cos \delta \ . \tag{54}$$

with $n_1 \cong n_2$,

$$\partial(\theta_2 - \theta_1)/\partial t = \partial\delta/\partial t = -2eV/\hbar \ . \tag{55}$$

relative phase of the probability amplitudes vary as

$$\delta(t) = \delta(0) - (2eVt/\hbar) \ . \tag{56}$$

$$J = J_0 \sin [\delta(0) - (2eVt/\hbar)] \ . \tag{57}$$

The phase is depending on time.

The current oscillates with frequency

$$\omega = 2eV/\hbar \ . \tag{58}$$

This is the **ac Josephson effect**. A dc voltage of 1 μV produces a frequency of 483.6 MHz. The relation (58) says that a photon of energy $\hbar\omega = 2eV$ is emitted or absorbed when an electron pair crosses the barrier.

Macroscopic Quantum Interference.

We consider two Josephson junctions in parallel, as in Fig. 25.

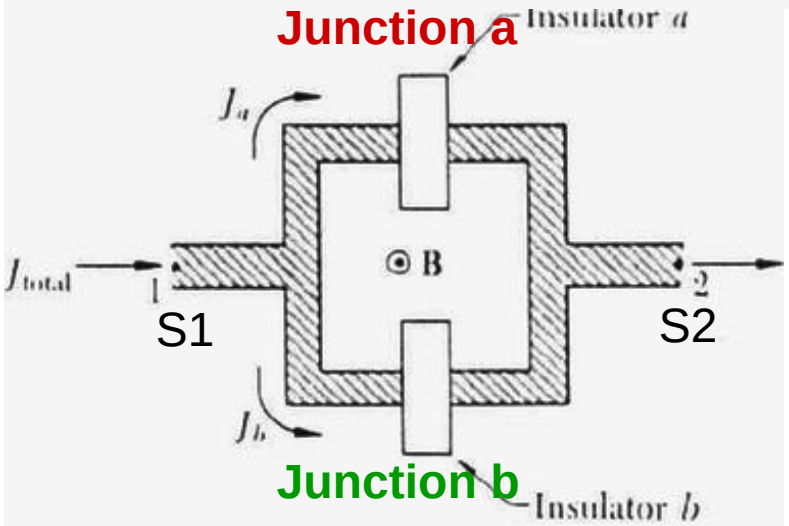

Figure 25 The arrangement for experiment on macroscopic quantum interference. A magnetic flux Φ passes through the interior of the loop.

Now let the flux Φ pass through the interior of the circuit. By (59), $\delta_b - \delta_a = (2e/\hbar c)\Phi$, or

$$\delta_b = \delta_0 + \frac{e}{\hbar c}\Phi \; ; \qquad \delta_a = \delta_0 - \frac{e}{\hbar c}\Phi \; . \quad (60)$$

The total current is the sum of J_a and J_b.

$$J_{\text{Total}} = J_a + J_b = J_0\left\{\sin\left(\delta_0 + \frac{e}{\hbar c}\Phi\right) + \sin\left(\delta_0 - \frac{e}{\hbar c}\Phi\right)\right\} = 2(J_0 \sin \delta_0)\cos\frac{e\Phi}{\hbar c} \; .$$

current varies with Φ and has maxima when

$$e\Phi/\hbar c = s\pi \; , \qquad s = \text{integer} \; . \quad (61)$$

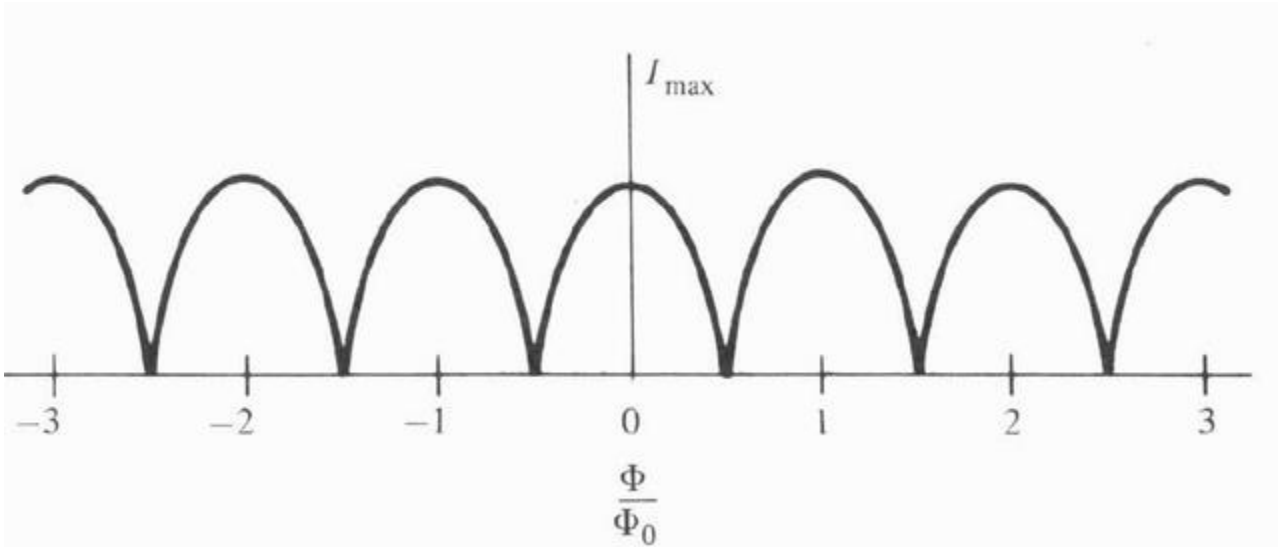

FIGURE 6-5
Dependence of maximum supercurrent through symmetrical two-junction superconducting interferometer (SQUID), shown schematically in Fig. 6-4.

Double slit diffraction pattern for two tunnel junctions

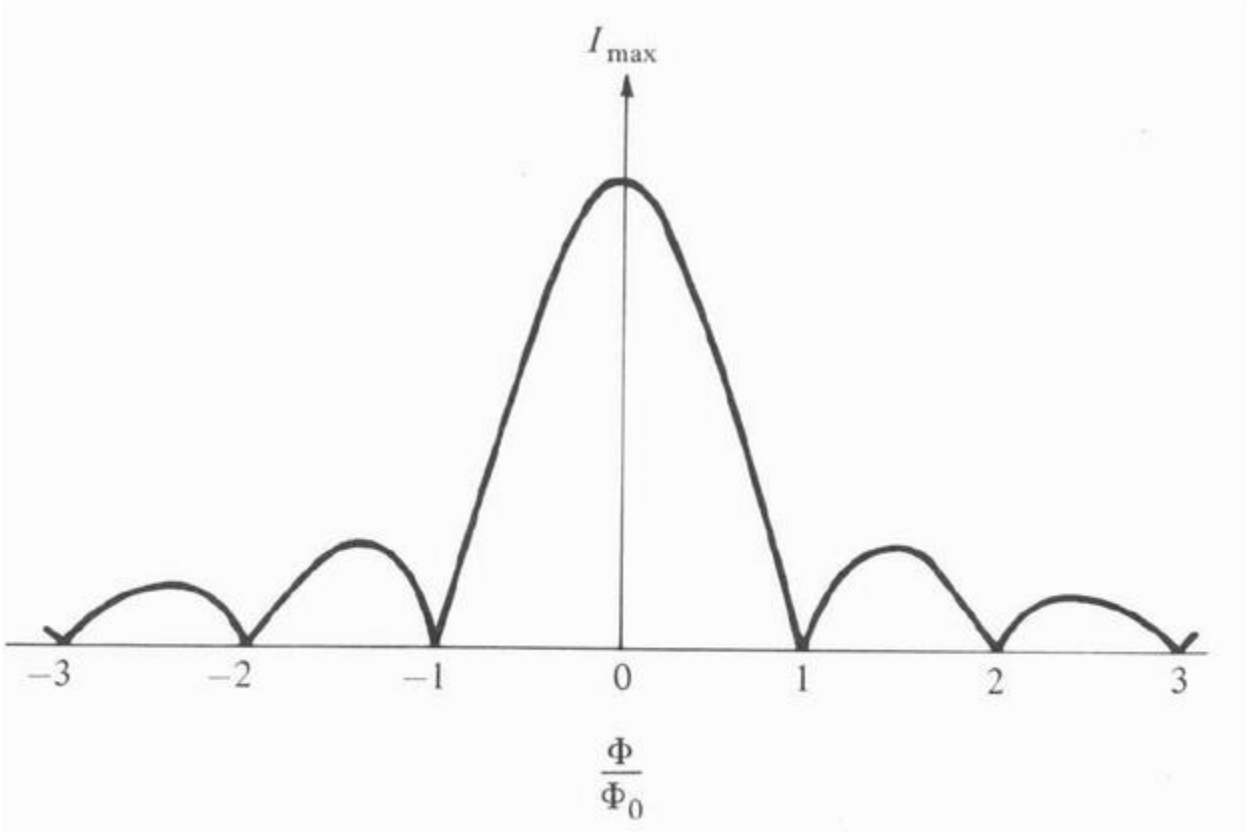

FIGURE 6-3
Dependence of maximum supercurrent through a Josephson junction upon the flux threading the junction. The resemblance to the "single-slit" diffraction pattern of optics is evident.

Single slit diffraction for single tunnel junction

The periodicity of the current is shown in Fig. 26.

1. The short period variation is produced by interference from the two junctions, as predicted by (61).
2. The longer period variation is a diffraction effect and arises from the finite dimensions of each junction

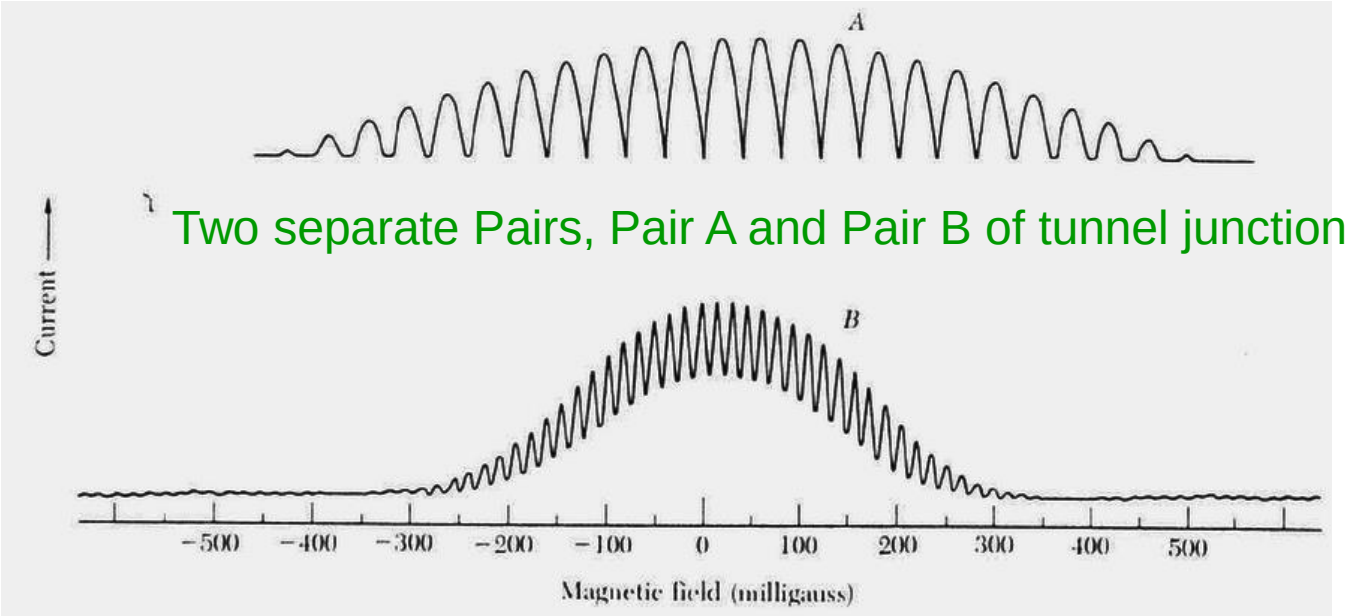

Two separate Pairs, Pair A and Pair B of tunnel junctions

Figure 26 Experimental trace of J_{max} versus magnetic field showing interference and diffraction effects for two junctions *A* and *B*. The field periodicity is 39.5 and 16 mG for *A* and *B*, respectively. Approximate maximum currents are 1 mA (*A*) and 0.5 mA (*B*). The junction separation is 3 mm and junction width 0.5 mm for both cases. The zero offset of *A* is due to a background magnetic field. (After R. C. Jaklevic, J. Lambe, J. E. Mercereau and A. H. Silver.)

The Discovery of Superconductivity

- Early 90's -- elemental SP metals like Hg, Pb, Al, Sn, Ga, etc.
- Middle 90's -- transitional metals, alloys, and compounds like Nb, NbN, Nb_3Sn, etc.
- Late 90's -- in perovskite oxides

Table 2 Superconductivity of selected compounds

Compound	T_c, in K	Compound	T_c, in K
Nb_3Sn A-15	18.05	V_3Ga	16.5
Nb_3Ge	23.2	V_3Si	17.1
Nb_3Al	17.5	$YBa_2Cu_3O_{6.9}$ HTSC	90.0
NbN B1	16.0	Rb_2CsC_{60}	31.3
K_3C_6O	19.2	La_3In	10.4

Superconductivity tunneling into the A-15 compounds

A-15 compound A_3B, with T_c = 15-23 K

With three perpendicular linear chains of ***A*** atoms on the cubic face, and B atoms are at body centered cubic site

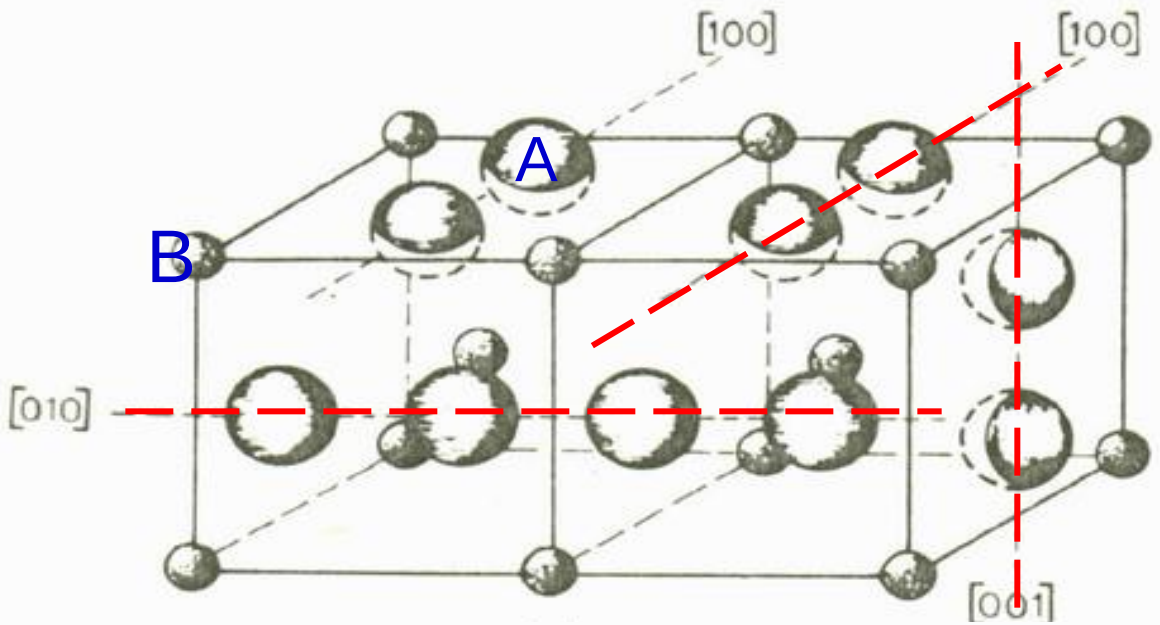

FIG. 34. (a) The position of A and B atoms in the unit cell of an A_3B compound possessing the β-W structure. (b) The fermi surface of an A_3B compound in the tight binding, nearest neighbors approximation. There are three degenerate bands corresponding to electrons localized on the three families of chains. (c) The first Brillouin zone (BZ) of the β-W lattice. The high symmetry points (Γ, X, M, R) and the high symmetry lines (Δ, Σ, Λ, Z, S, T) are indicated.

1973 Nb_3Ge, 23K !

Low temperature Superconductors

-- Mediated by Electron phonon coupling

-- McMillian formula for T_c

$$T_c = \frac{\Theta_D}{1.45} \exp\left\{ - \left[\frac{(1+\lambda_{ep})}{\lambda_{ep} - \mu^*(1+0.62\lambda_{ep})} \right] \right\}$$

λ : electron phonon coupling constant

μ^* : Coulomb repulsion of electrons

$\lambda \propto N(0) < I^2 > / \omega^2$

Are electrons or phonons more important?

Superconductivity tunneling into the A-15 compounds

PHYSICAL REVIEW B VOLUME 23, NUMBER 7 1 APRIL 1981

Superconducting tunneling into the *A*15 Nb_3Al thin films

J. Kwo and T. H. Geballe*
Department of Applied Physics, Stanford University, Stanford, California 94305
(Received 1 October 1980)

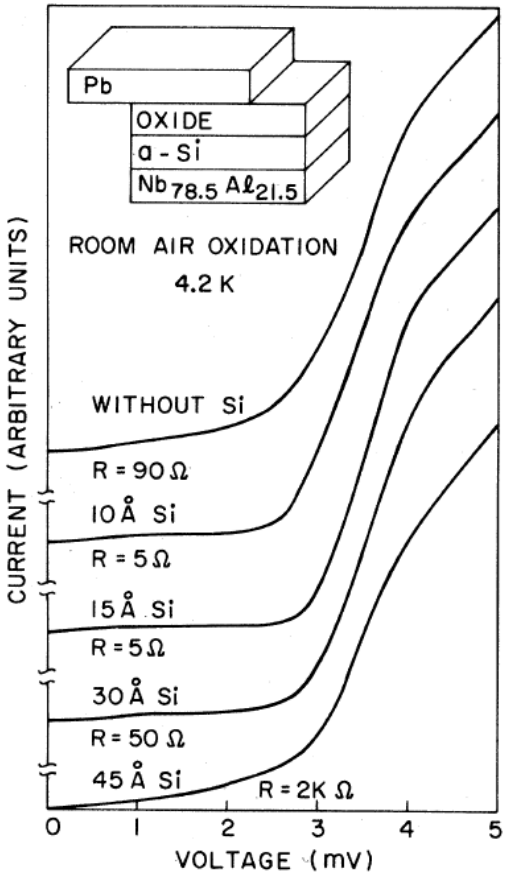

FIG. 1. Current-voltage characteristics at 4.2 K of *A*15 Nb-Al (of 21.5 at.% Al) tunnel junctions with the thickness of the *a*-Si overlay varying from 0 to 45 Å.

Native Oxide of Nb, no good!

Use of a thin amorphous
Si oxide 15A thick, excellent !

Tunneling as a materials diagnosis

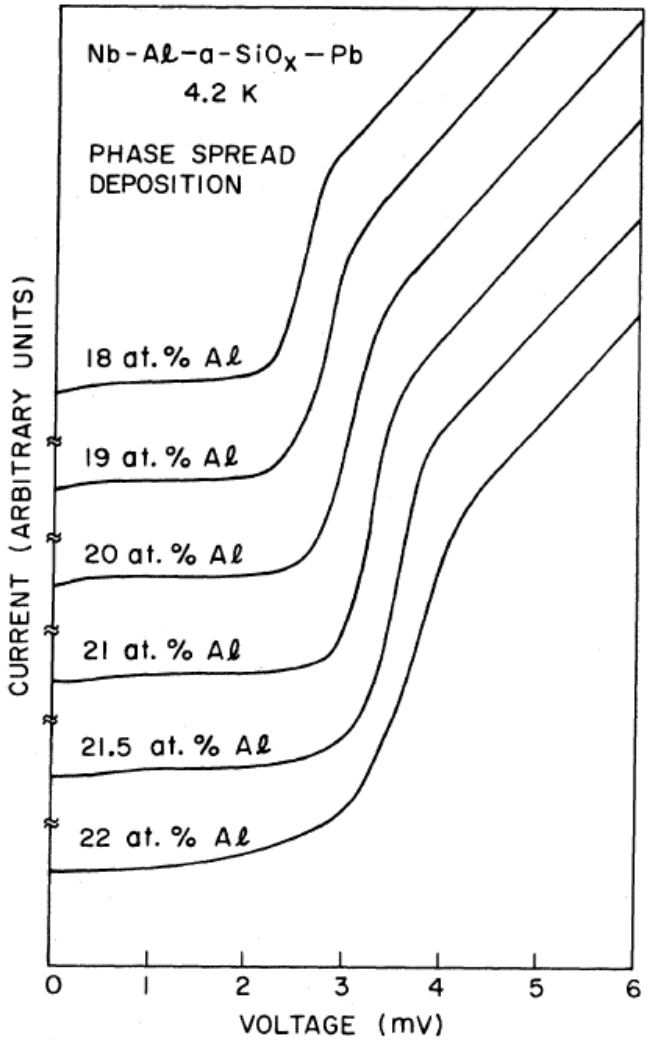

FIG. 2. Current voltage characteristics at 4.2 K of a series of *A*15 Nb-Al junctions obtained from a phase-spread deposition at 950 °C. The thickness of the *a*-Si overlay is of 15 Å. The *A*15 phase boundary is at 21.8 at.% Al.

Self-Epitaxial Growth

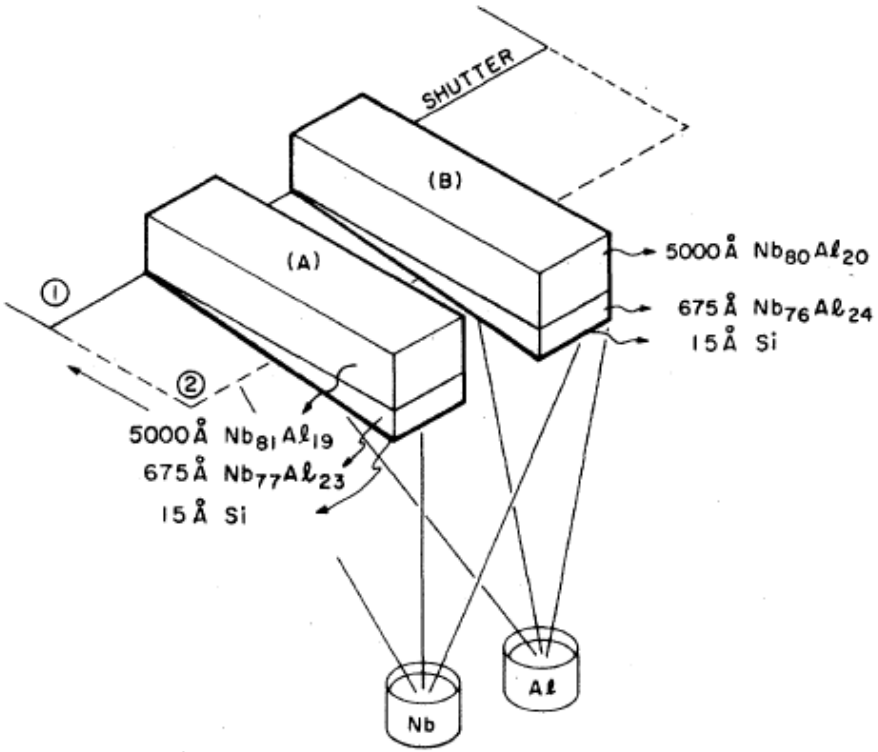

FIG. 3. Configuration for the self-epitaxy deposition in the constant phase direction at 950 °C. The epitaxial layer thickness is varying from zero at one end of the 10 substrates to 675 Å at the other end.

The use of tunneling to probe the highest T_c layer via self-epitaxial growth

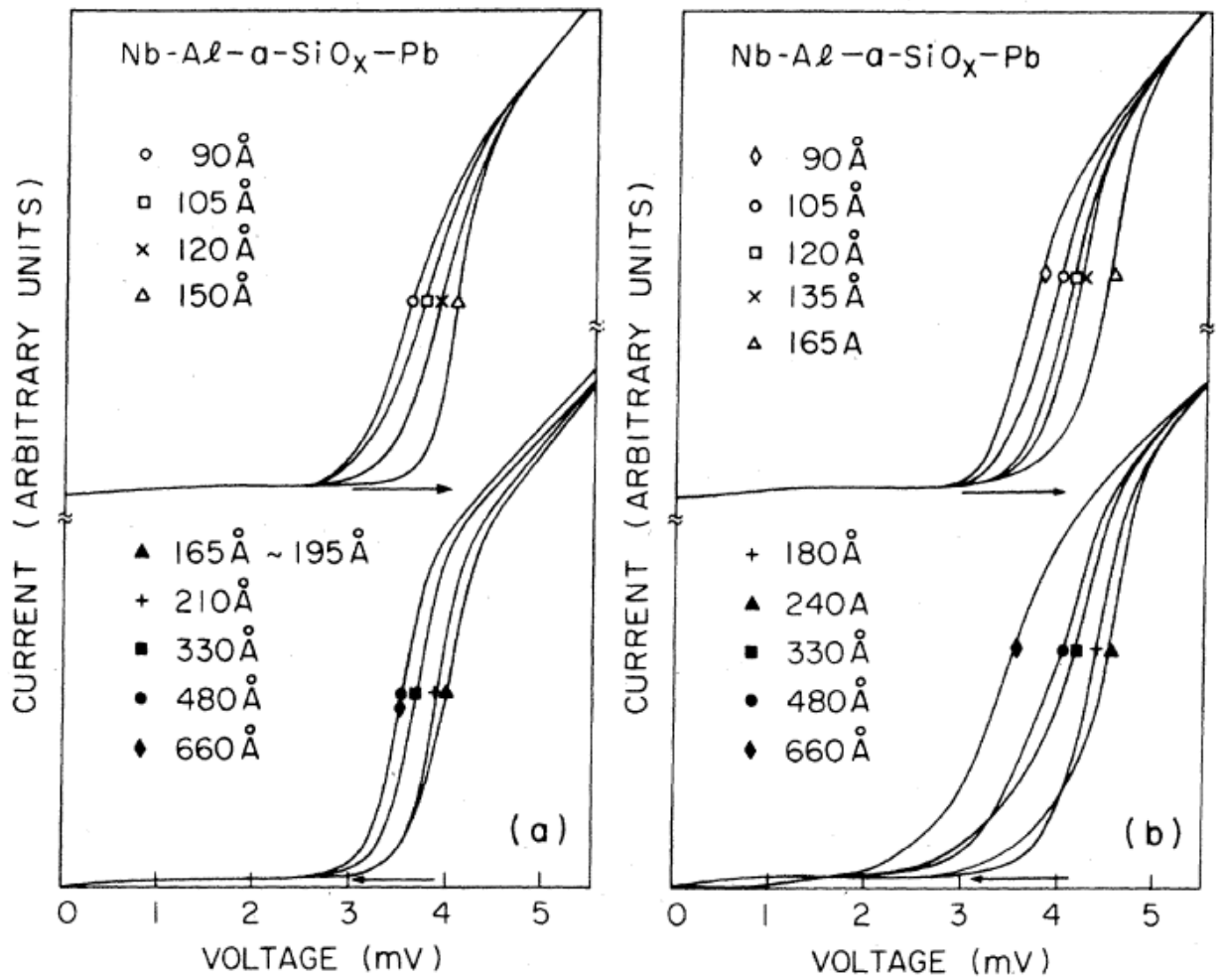

FIG. 4. (a) Current vs voltage at 4.2 K of a series of tunnel junctions on the (*A*)-row self-epitaxial samples with epilayer thickness *d* systematically increasing from 90 to 660 Å. The composition of the epilayer is of 23 at.% Al. (b) The same for the (*B*)-row self-epitaxial sample. The composition of the epilayer is of 24 at.% Al.

Electron –phonon coupling strength vs composition

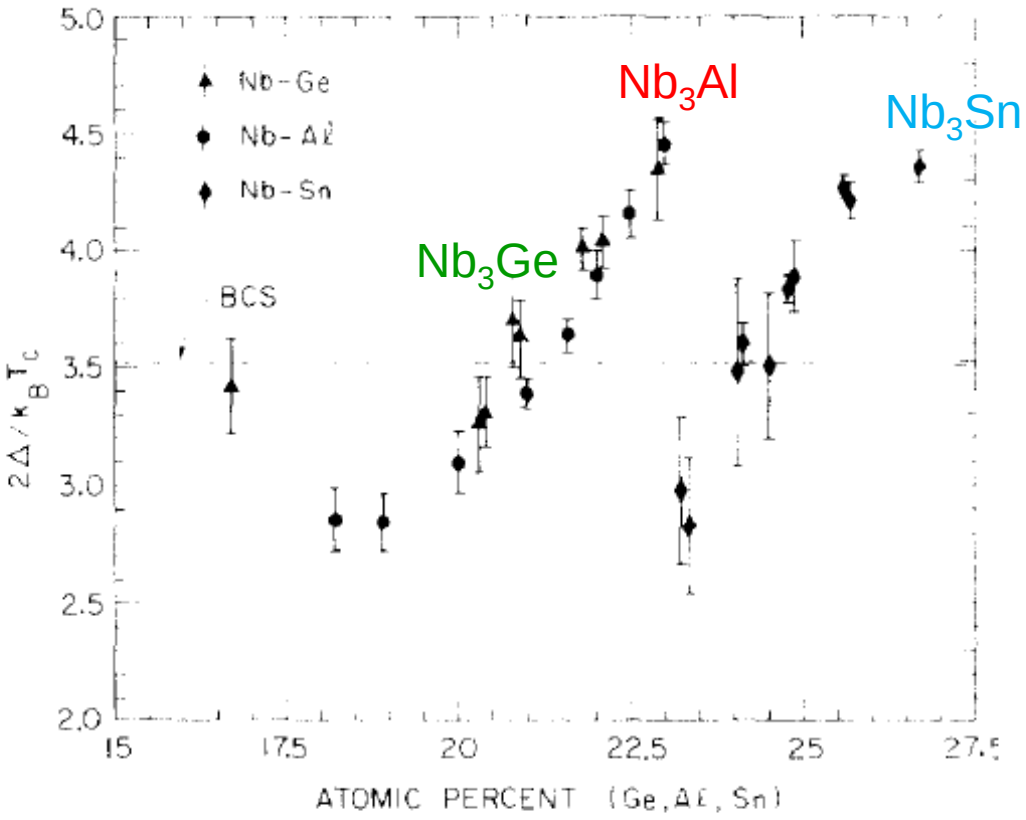

Fig. 2. The variation with composition of the electron–photon coupling strength $2\Delta/k_B T_c$ for the A15 Nb_3Sn, Nb_3Al, and Nb_3Ge. The data are from Rudman et al. [20], Kwo et al. [10], and Khilstrom et al. [11], respectively.

The origin of this dramatic change of the electron-phonon coupling strength of Nb_3Al with the composition approaching the $A15$ phase boundary is not well understood. An insight can be gained from referring to the analytical formula by Kresin *et al.*,[21]

$$2\Delta/k_B T_c = 3.53[1 + 5.3(T_c/\omega_0)^2 \ln(\omega_0/T_c)] \ ,$$

which expresses the enhancement of the coupling strength $2\Delta/k_B T_c$ as an explicit function of the ratio T_c/ω_0, where ω_0 is a characteristic Einstein phonon frequency. An analysis based on this formula shows that a change in the $2\Delta/k_B T_c$ ratio from BCS-like to a value as large as 4.4 requires a substantial increase in T_c/ω_0. Since T_c varies only modestly, from 14.0 to 16.4 K, the occurrence of phonon-mode softening, i.e., a smaller ω_0, appears necessary to account for the large increase in T_c/ω_0. The most direct proof of this supposition is to examine the $\alpha^2 F(\omega)$ functions obtained experimentally from tunneling densities of states.

E. Tunneling density of states and $\alpha^2F(\omega)$

The dynamic resistance dV/dI as a function of the bias voltage has been measured for several Nb-Al junctions of importance. Data of the superconducting state were taken at 1.5 K with a magnetic field ~1 kG applied to quench the superconductivity in Pb. Throughout the data reduction, a constant excess conductance, of about 2–5% of the normal-state conductance, was subtracted out from both the superconducting and the normal-state tunneling conductance. The energy gap Δ was determined experimentally with the aid of Bermon's table.[22] The reduced tunneling density of states $R(\omega) = N_{expt}(\omega)/N_{BCS}(\omega) - 1$ was then calculated. Figure 6 shows

- Reduced tunneling density of states $R(\omega)$

  $R(\omega) = N_{exp}(\omega) / N_{BCS}(\omega) - 1$

- *Use $R(\omega)$ and Δ to deduce to $\alpha^2F(\omega)$*

  by the MR inversion program to get λ and μ^*

- *by the MMR inversion program to include a nornal proximity layer*

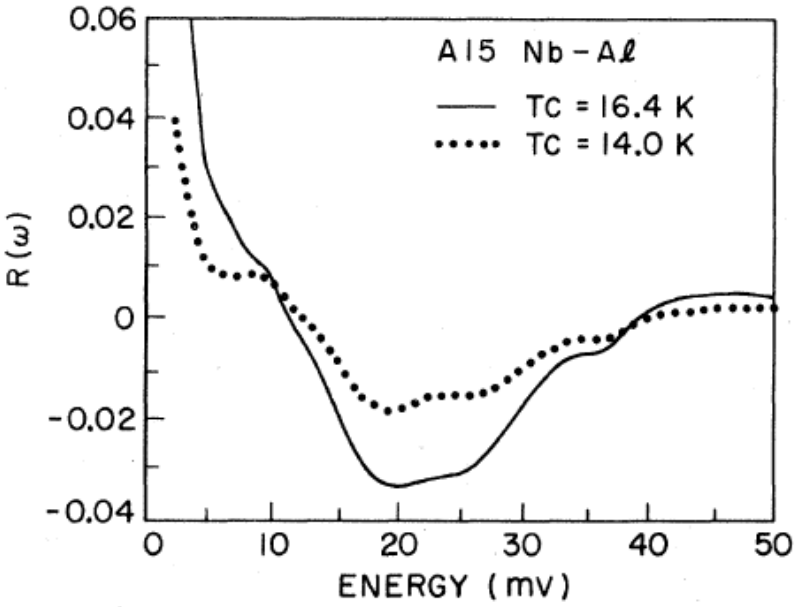

FIG. 6. Reduced tunneling density of states $R(\omega)$ vs energy above the gap for the two Nb-Al junctions of $T_c = 16.4$ K, $\Delta = 3.15$ meV and $T_c = 14.0$ K, $\Delta = 2.15$ meV, respectively.

The electron-phonon spectral function $\alpha^2F(\omega)$ has been generated from the input data of $R(\omega)$ and Δ by the gap-inversion analysis for these two junction The initial method employed was the conventional McMillan-Rowell inversion program.[24] For the jun tion with a T_c of 16.4 K and a Δ of 3.15 meV, that analysis gives a value of only 0.6 for the electron-phonon interaction parameter λ and a negative valu ~ -0.10 for the effective Coulomb pseudopotential μ^*. The calculated T_c from these parameters is thu less than 10 K. Perhaps the most unphysical result using that analysis is that a high-energy cutoff of le than 30 meV had to be imposed to prevent the iter tive solutions from becoming unstable. The structu between 20 and 40 meV, as associated with the Al phonons, was then left out entirely. Furthermore, a shown in Fig. 7, there is a large positive offset between the experiment and the calculated $R(\omega)$'s.

modified McMillan-Rowell (MMR) inversion analysis based on the model of proximity-effect tunneling, proposed by Arnold[26] and implemented by Wolf *et al.*,[27] has permitted an improved description, i.e., more self-consistent, of the tunneling data of such Nb and Nb_3Sn junctions within the conventional framework of the strong-coupling theory.[28,29] In this model a thin layer of weakened superconductivity is proposed to exist between the insulating oxide and the base electrode, and it is characterized by a constant pair potential $\Delta_n << \Delta_s$ and a thickness of $d_n << \xi$.

It is plausible that a thin proximity layer exists between the Nb_3Al film and the *a*-Si oxide barrier. It

With no *a priori* knowledge about this promixity layer, we approximate it with $\Delta_n = 0$. The tunneling density of states is then, as shown in Ref. 26, dependent on two additional parameters, $2d_n/\hbar v_F^*$ and d_n/l, where d_n, v_F^*, and l are the thickness, the renormalized Fermi velocity, and the mean free path of the promiximity layer, respectively.

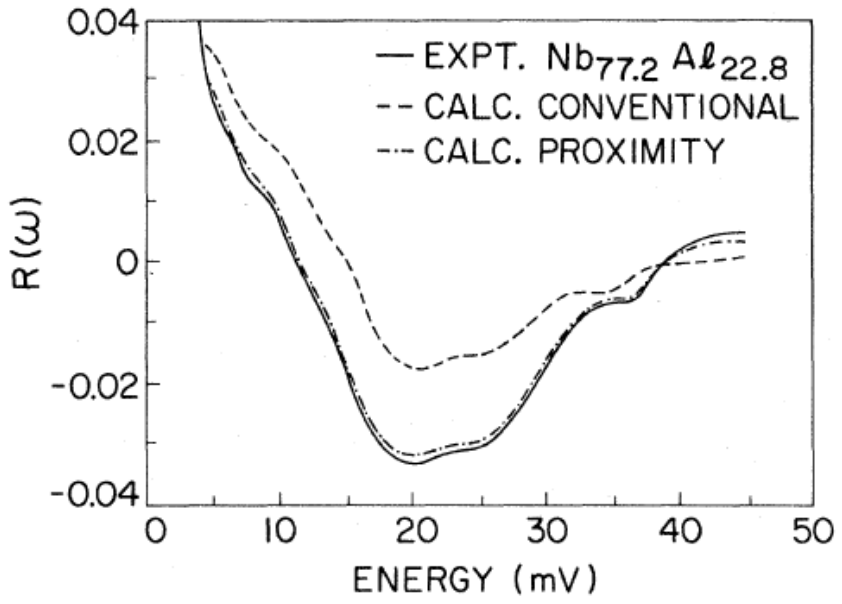

FIG. 7. The experimental and calculated tunneling densities of states $R(\omega)$'s from both conventional and proximity inversion analysis for the $A15$ Nb-Al junction of 22.8 at.% Al with $T_c = 16.4$ K and $\Delta = 3.15$ meV.

reduced tunneling density of states $R(\omega) = N_{\text{expt}}(\omega)/N_{\text{BCS}}(\omega) - 1$ was then calculated. Figure 6 shows the $R(\omega)$'s for two particular junctions. One is a relatively weak coupled superconductor, with a T_c of 14.0 K and a gap of 2.15 meV; the other is strong coupled, of larger Al composition by 1.3 at.%, with a higher T_c at 16.4 K and a gap of 3.15 meV. A reduction in the magnitude of $R(\omega)$ is found as the Al composition is reduced, indicating a weakening in the electron-phonon coupling strength. However, the overall shapes of the two $R(\omega)$'s are rather similar, and there is no dramatic change in the positions of structures induced by phonons. Similar behavior is found in the tunneling densities of states of Nb_3Sn junctions of different T_c's and coupling strength.[23]

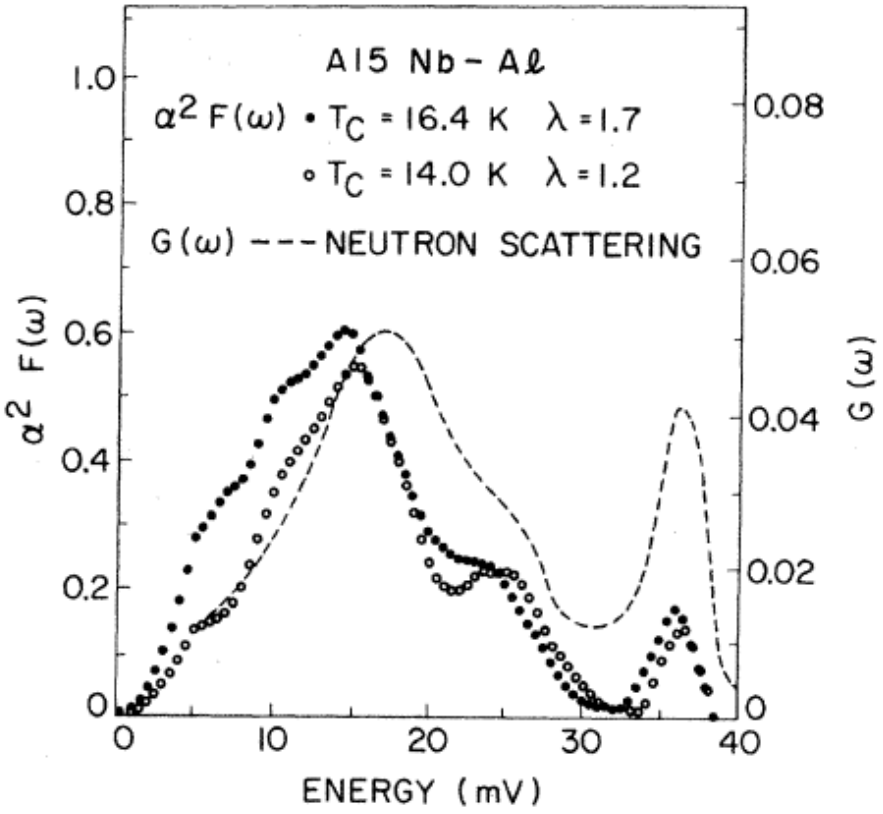

FIG. 8. The electron phonon spectral functions $\alpha^2F(\omega)$ for two Nb-Al junctions with $2\Delta/k_BT_c$ of 3.6 and 4.4. The data of the neutron scattering function $G(\omega)$ are after Schweiss *et al.* (Ref. 9).

features of the $\alpha^2F(\omega)$ functions of these two junctions are quite similar, with a slight reduction of about 10% in the $\alpha^2F_{\max}$ for the lower-T_c one. However the strong-coupled and high-T_c junction shows a pronounced enhancement in the weightings of the low-frequency phonons, leading to smaller values of the frequency moments. In fact, the significant reduction of λ, from 1.7 to the 1.2 found for the lower-T_c junction, is mainly from the stiffening of phonons; i.e., $\langle\omega^2\rangle$ is larger by 20%. The $\alpha^2F(\omega)$

TABLE I. A summary of the parameters from the proximity inversion analysis of two *A*15 Nb-Al junctions and one Nb_3Sn junction.

	Composition	T_c (K) (expt)	Δ (meV) (expt)	$\frac{2\Delta}{k_B T_c}$ (expt)	λ	μ^*	$\omega_{\log}^{b}$ (meV)	$\langle\omega\rangle^{b}$ (meV)	$\langle\omega^2\rangle^{b}$ $(meV)^2$	T_c (K)[c] (calc)	$\frac{2\Delta}{k_B T_c}$ (calc)	$\frac{2d_n}{\hbar v_F^*}$ $(meV)^{-1}$	$\frac{d_n}{l}$
*A*15 Nb-Al	21.5 at.% Al	14.0 ± 0.2	2.15	3.56	1.2 ± 0.05	0.13 ± 0.01	11.2	13.3	226	11.7	3.8	0.0055	0.065
	22.8 at.% Al	16.4 ± 0.1	3.15	4.45	1.7 ± 0.05	0.15 ± 0.02	9.5	11.4	181	15.1	4.3	0.006	0.055
*A*15 Nb-Sn	25.0 at.% Sn	17.7 ± 0.1	3.25	4.26	1.8 ± 0.15	0.16 ± 0.03	10.8	13.1	226	16.7	4.25	0.0097	0.13

$$T_c = \frac{\Theta_D}{1.45} \exp\left\{ - \left[\frac{(1+\lambda_{ep})}{\lambda_{ep} - \mu^*(1+0.62\lambda_{ep})} \right] \right\}$$

to the analytical formula by Kresin *et al.*,[21]

$$2\Delta/k_B T_c = 3.53[1 + 5.3(T_c/\omega_0)^2 \ln(\omega_0/T_c)] \ ,$$

which expresses the enhancement of the coupling strength $2\Delta/k_B T_c$ as an explicit function of the ratio T_c/ω_0, where ω_0 is a characteristic Einstein phonon frequency.

[a] $\lambda = 2 \int d\omega \omega^{-1} \alpha^2 F(\omega).$

[b] $\omega_{log} = \exp\left[\frac{2}{\lambda} \int d\omega \omega^{-1} \ln\omega \alpha^2 F(\omega) \right]$.

[c] $T_c = \frac{\langle\omega\rangle}{1.2} \exp\left[\frac{-1.04(1+\lambda)}{\lambda - \mu^*(1+0.62\lambda)} \right]$, see Ref. 30.

$\lambda = N(0)\langle I^2 \rangle / M \langle \omega^2 \rangle$

The electron–phonon coupling constant λ can be expressed, according to McMillan, as a product of $N^b(0)\langle I^2\rangle/M\langle\omega^2\rangle$ where $N^b(0)$ and $\langle I^2\rangle$ are the electronic band density of states and the electron–phonon matrix element evaluated over the Fermi surface, respectively. The electronic parameter $N^b(0)$ can be estimated from the renormalized density of states $N^*(0)$ by specific heat experiments or from upper critical field analysis, given that the $(1+\lambda)$ factor is known from tunneling. Systematic variations of these

(1) or (2)

$$C_{el} = 1/3\ \pi^2 N(0) K_B^2\ T$$

$$N^b(0)\left[\frac{\text{states}}{\text{eV spin unit cell}}\right] = \frac{17.8}{1+\lambda}\gamma^{*M}\left[\frac{\text{mJ}}{\text{cm}^3\text{K}^2}\right],$$

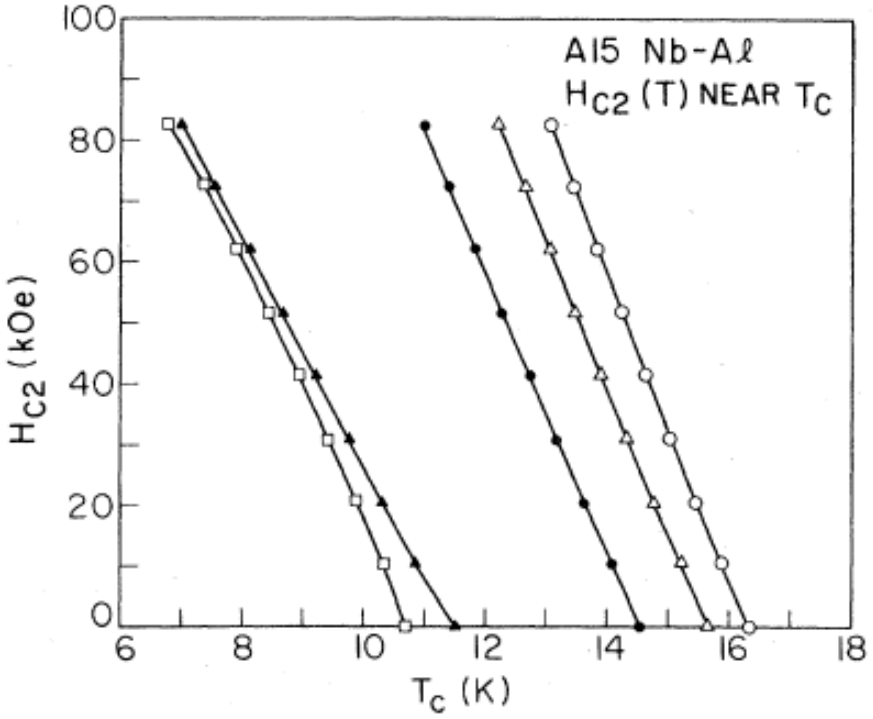

FIG. 1. Representative critical-field data near T_c of the $A15$ Nb-Al films measured. The lines drawn through data points are intended to serve only as a guide to the eye.

Based on the data of the critical-field slope near T_c, the general procedure of evaluating various superconducting and normal-state parameters including $N^b(0)$ is well formulated.[20] Briefly, the slope of critical field near T_c including corrections for the electron-phonon interaction can be written as[21]

$$\left.\frac{dH_{c2}}{dT}\right|_{T_c} = \eta_{H_{c2}}(T_c)\left[9.55\times10^{24}\gamma^{*2}T_c\left(\frac{n^{3/2}S}{S_F}\right)^{-2} + 5.26\times10^{4}\gamma^{*}\rho(\Omega\,\mathrm{cm})\right]\times[R(\gamma_{tr})]^{-1}\ \mathrm{Oe/K}\ ,$$

The electron–phonon spectral function $\alpha^2F(\omega)$

Nb_3Sn

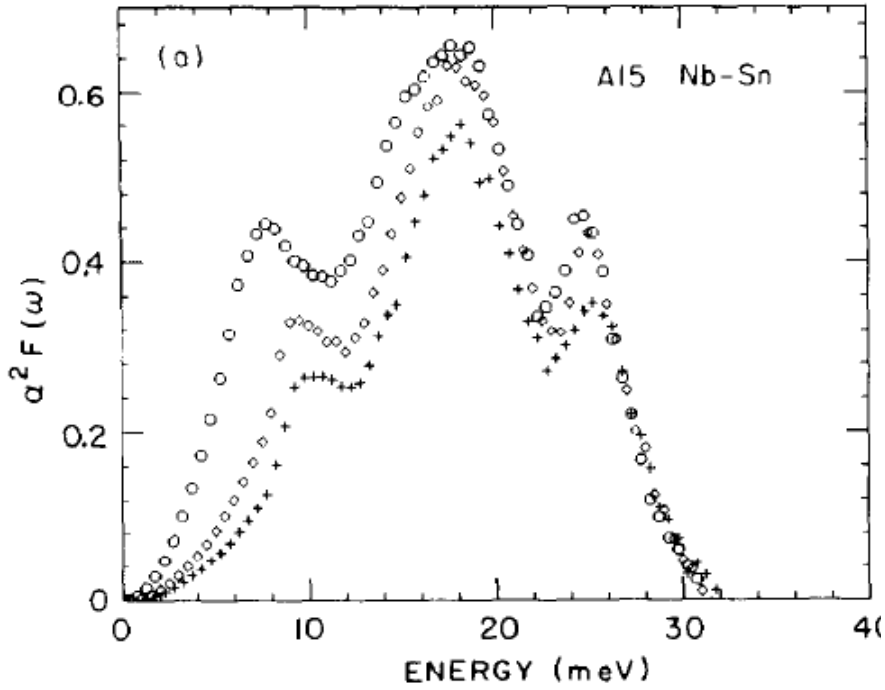

Nb_3Ge